An fNIRS-Based Motor Imagery BCI for ALS: A Subject-Specific Data-Driven Approach

S. M. Hosni, S. B. Borgheai, *Member, IEEE,* J. McLinden, *Member, IEEE,* and Y. Shahriari*, *Senior Member, IEEE*

Abstract*—*Objective: **Functional near-infrared spectroscopy (fNIRS) has recently gained momentum in research on motor-imagery (MI)-based brain-computer interfaces (BCIs). However, strikingly, most of the research effort is primarily devoted to enhancing fNIRS-based BCIs for healthy individuals. The ability of patients with amyotrophic lateral sclerosis (ALS), among the main BCI end-users to utilize fNIRS-based hemodynamic responses to efficiently control an MI-based BCI, has not yet been explored. This study aims to quantify subject-specific spatio-temporal characteristics of ALS patients' hemodynamic responses to MI tasks, and to investigate the feasibility of using these responses as a means of communication to control a binary BCI.** ***Methods*****: Hemodynamic responses were recorded using fNIRS from eight patients with ALS while performing MI-Rest tasks. The generalized linear model (GLM) analysis was conducted to statistically estimate and evaluate individualized spatial activation. Selected channel sets were statistically optimized for classification. Subject-specific discriminative features, including a proposed data-driven estimated coefficient obtained from GLM, and optimized classification parameters were identified and used to further evaluate the performance using a linear support vector machine (SVM) classifier.** ***Results*****: Inter-subject variations were observed in spatio-temporal characteristics of patients' hemodynamic responses. Using optimized classification parameters and feature sets, all subjects could successfully use their MI hemodynamic responses to control a BCI with an average classification accuracy of 85.4%±9.8%.** ***Significance*****: Our results indicate a promising application of fNIRS-based MI hemodynamic responses to control a binary BCI by ALS patients. These findings highlight the importance of subject-specific data-driven approaches for identifying discriminative spatio-temporal characteristics for an optimized BCI performance.**

Index Terms*—*Amyotrophic lateral sclerosis (ALS), brain-computer interface (BCI), functional near-infrared spectroscopy (fNIRS), subject-specific data-driven approach.

I. Introduction

BRAIN-COMPUTER interface (BCI) systems can extend the frontiers of human communication to the neural level by encoding discriminative features of brain responses during certain mental tasks into control signals that can be used for communication. Probing the brain during motor imagery (MI) tasks in which the subject imagines moving a limb has been extensively researched in the BCI domain, as the cognitive execution of movement induces neural responses that overlap with actual motor execution (ME) [1], [2]. MI has naturally been adopted as a BCI paradigm suitable for people with severe motor disabilities, including amyotrophic lateral sclerosis (ALS), who are incapable of any voluntary ME tasks.

*Yalda Shahriari, Sarah M. Ismail Hosni, Seyyed Bahram Borgheai, and John McLinden are with the Department of Electrical, Computer & Biomedical Engineering, University of Rhode Island (URI), RI 02881, USA. E-mail address: yalda_shahriari@uri.edu (*Corresponding author).

MI responses can be triggered endogenously, as they do not rely on any external stimulus. This is vital in advanced ALS, when patients lose most voluntary muscle control, including eye-gaze control. MI is, therefore, a great candidate for BCI systems, as it offers intentionally-generated, decodable brain characteristics that can be independently controlled by users. MI tasks for BCI systems offer a wide range of potential clinical applications, as they offer a non-muscular neurorehabilitation technique through the direct activation of MI neural circuits in order to enhance motor and cognitive recovery for patients with severe neuromuscular disorders and brain injuries [3]. These clinical research areas further provide insight into disease-specific neural markers, which advance diagnosis and treatment techniques in addition to improving BCIs through optimal designs as practical assistive technologies.

To date, electroencephalography (EEG) has been the most extensively researched non-invasive neuroimaging modality in MI-based BCIs, primarily due to its non-invasiveness, low-cost, portability, and instantaneous measure of neural activity. In particular, MI modulates oscillatory variations in EEG sensorimotor rhythms (SMR), including the μ (8–12 Hz) and β (13–30 Hz) frequency bands, known as event-related desynchronization (ERD) and event-related synchronization (ERS) [1]. SMR-based BCI is established for both healthy and ALS users [4], [5]. However, despite existing promising results, many studies have shown that SMR-based BCI end-users do not consistently achieve satisfactory performance levels, especially without extensive training [6]. Insights from our studies and others characterizing ALS-specific electrophysiological alterations point to an overall reduction in ERD during motor imagery, generally associated with ALS motor impairments [7], [8], which raises questions about the feasibility of relying solely on EEG to control the BCIs for these cohorts.

Functional near-infrared spectroscopy (fNIRS) is another non-invasive neuroimaging modality that has been used in the BCI domain for several years. fNIRS relies on optical technology, using near-infrared spectrum light to monitor the hemodynamic responses evoked by neural activity by measuring changes in oxygenated hemoglobin (HbO2) and deoxygenated hemoglobin (HbR) concentrations from the cortical surface [9]. These variations in fNIRS measurements reflect the increased or decreased blood supply to active cortical areas due to neurovascular coupling and correlate with the blood oxygen level-dependent (BOLD) signal recorded through functional magnetic resonance imaging (fMRI) [10]. As fNIRS offers a unique trade-off between EEG's high temporal resolution and fMRI's high spatial resolution, its portability, low cost, metabolic-based specificity, and robustness to various types of artifacts when compared to EEG, it is a good candidate for BCI applications. In addition, fNIRS allows for a less

restrictive natural setting that does not require patients to lay flat or to be exposed to loud fMRI noises. Therefore, fNIRS is important to advance BCI research for ALS towards improved efficacy and a better understanding of brain functionality.

The feasibility of using fNIRS as a BCI control signal was first tested by Coyle et al. [2], who used a simple threshold technique (i.e., mean HbO2) to classify MI vs. Rest with 75% average accuracy. Sitaram et al. [11] confirmed fNIRS as a promising BCI neuroimaging modality, using mean HbO2 and HbR amplitude changes to distinguish left-hand MI (LMI) from right-hand MI (RMI), with an average offline accuracy of 73% and 89% with support vector machines (SVM) and hidden Markov models (HMM), respectively. The first online fNIRS MI-based BCI, "Mindswitch," was presented as a basic BCI system allowing users to control an "On/Off" switch in almost one minute per selection. The users modulated variations in mean HbO2 over their motor cortices by imagining squeezing a softball, controlling the system with an online accuracy of 50%-85% [12]. Various levels of complexity in MI tasks were investigated by Holper et al. [13]. Through a cross-validation process and using Fisher's linear discriminant analysis (FLDA), subject-specific parameters were selected involving the best performing channel, the best analysis time interval, and a set of up to four features, including mean HbO2, variance, skewness, and kurtosis. Simple and complex MI tasks were distinguished, with an average classification accuracy of 81%. Naseer et al. [14] showed that including the slope along with mean HbO2 can significantly increase accuracy, as can restricting the classification window to [2-7] sec relative to the imagination onset within a 10-sec task. The authors discriminated LMI from RMI with an average accuracy of 87% using linear discriminant analysis (LDA). In another study [15], they also demonstrated the feasibility of adding mental arithmetic (MA) to LMI/RMI tasks in a three-class BCI and thereby increase the number of commands. Their classifier discriminated between the three classes, with an average offline accuracy of 75.6% using a reduced time window [2-7] sec after imagination onset.

Research investigating the performance of fNIRS-based BCIs in ALS patients is scarce. Naito et al. [16] were the first to investigate fNIRS-based BCI for ALS in 2007. MA and mental singing cognitive activities were used to answer a series of "yes/no" questions by inducing brain activity variations reflected in cortical blood volume changes detected with near-infrared light. To assess patients' ability to modulate cerebral blood volume changes with intention, their detected light intensity signals were analyzed for the separability of "yes" and "no" patterns, i.e., patients were categorized into two groups, based on the separability of their responses. The average classification accuracy was 80% for patients in the higher separation group but did not exceed 42% for the other group. However, the proposed system only reached acceptable accuracies for 70% of ALS participants and only 40% of the locked-in patients. One possible explanation for the limited applicability of their approach is a lack of subject-specific features. The authors employed the same features for all ALS subjects and did not accommodate for possible inter-individual hemodynamic response variabilities. Similar results were demonstrated in a case study of a completely locked-in syndrome (CLIS) patient with ALS [17] by classifying hemodynamic responses to correct and incorrect statements, with classification accuracy significantly above chance.

Despite a considerable number of studies devoted to the enhancement of MI-based BCIs relying on fNIRS techniques, no study confirms that ALS patients can use MI-hemodynamic responses (MI-HR) to control a BCI. The inter-individual variabilities of fNIRS-based hemodynamic responses remain a challenge further augmented for ALS patients with potentially altered responses due to underlying neurological conditions.

This study aims to quantify the subject-specific spatio-temporal characteristics of ALS patient's MI-HR measured using fNIRS and to assess the feasibility of using MI-HR to control a binary BCI in these cohorts. This paper focused on the classification of MI versus Rest to verify MI activation for ALS patients. The individualized spatio-temporal characteristics of MI (combined LMI and RMI) hemodynamic responses were characterized and used to optimize the classification parameters and feature sets. As the exact shape of MI-HR has not been yet evaluated for ALS, and given the potential contamination of fNIRS signals with physiological noise, the fNIRS-measured cortical activation of MI tasks was statistically estimated and verified using a generalized linear model (GLM) with respect to a canonical hemodynamic response function (*cHR*). To accommodate for atypical responses using the subject's individual patterns, we further proposed a data-driven estimated coefficient obtained from GLM as a novel feature to enhance classification performance. The performance of the binary BCI (MI vs. Rest) was finally evaluated through 5-fold cross-validation using an SVM classifier.

II. Methods

A. Participants

Eight ALS patients were recruited for our study (age: 57.9 ± 13.8 years, two females), with varying degrees of disability, assessed using the ALS functional rating scale-revised (ALSFRS-R: 18.2 ± 14.6) on a 48-point scale [18]. Three patients (ALS-1, ALS-2, and ALS-4) were completely dependent on mechanical ventilation, and had very low ALSFRS-R scores (0-7). These patients had no verbal communication abilities. The youngest (ALS-1) was in a late-stage locked-in state (LIS) with no objective means of communication, due to the loss of all muscle control, including eye movement. All participants except for ALS-6 were right-handed. ALS-8 was right-hand dominant, but could write with both hands. Table I shows the patients' demographics information. The study protocol was approved by the institutional review board (IRB) of the University of Rhode Island (URI), and written informed consents were provided either by each patient or their caregiver.

B. Data Acquisition and Experimental Protocol

fNIRS data were recorded using NIRScout (NIRx Inc.), with two near-infrared light wavelengths (760 nm and 850 nm) to acquire HbR and HbO2 responses, respectively. The signals were digitized at 15.6 Hz, and the optode montage was configured using 16 probes, eight sources, and eight detectors mounted on a standard EEG cap, with a separation distance of ~3 cm to maintain acceptable signal quality and sensing depth. The probe-layout resulted in 14 channels, as shown in (Fig. 1-left), following previous research, which commonly reports the engagement of the pre/frontal cortex in addition to the primary

TABLE I
PARTICIPANT'S DEMOGRAPHIC INFORMATION.

Participant No.	*Age*	*Sex*	*ALSFRS-R (max 48)*	*Disease Duration (years)*	*Handedness*
ALS-1	29	M	0	4	R
ALS-2	55	M	4	11	R
ALS-3	70	M	14	8	R
ALS-4	67	M	7	2	R
ALS-5	69	F	23	11	R
ALS-6	52	M	22	3	L
ALS-7	54	F	39	2	R
ALS-8	67	M	37	0.6	R
Mean±SD	57.9±13.8	-	18.2±14.6	5.2±4.2	-

motor cortex in MI-related tasks [19]. As depicted in Fig. 1-left, for simplicity, we used source (S) and detector (D) numbers to illustrate our probe-layout. The sources were located according to the 10-5 electrode placement system as follows—AF3 (S1), AF4 (S5), FCC5h (S3), FCC1h (S2), FCC2h (S6), FCC6h (S7), CCP3h (S4), and CCP4h (S8)—while the detectors were placed at AFF1 (D2), AFF2 (D6), F5 (D1), F6 (D5), FCC3h (D3), FCC4h (D7), CCP1h (D4), and CCP2h (D8). Four fNIRS channels covered the pre/frontal cortex (CH1, CH2, CH8, and CH9) associated with the pre/supplementary motor area (pre/SMA), involved in motor preparation. In the proximity of the primary motor cortex, ten channels (CH3, CH4, CH5, CH6, CH7, CH10, CH11, CH12, CH13, and CH14) were positioned to surround the standard C1, C2, C3, and C4 areas as reference points for hand MI-related activation of the motor cortex.

Data was recorded from ALS patients in their homes or care centers. Subjects who retained the ability to move their arms were instructed to relax their arms and avoid movement. The MI stimulation paradigm was designed using BCI2000 software. The recording session consisted of three runs separated by approximately five minutes of rest. During each run, the subject was instructed to respond to three types of visual cues presented on-screen with three types of mental motor activities: (a) left-hand motor imagery (LMI) when the cue appears on the left side of the screen; (b) right-hand motor imagery (RMI) when the cue appears on the right side of the screen; and (c) resting when the cue appears in the middle of the screen (Fig. 1-right). Each run consisted of 10 trials for each type of MI task randomly, with Rest trials in between (20 MI trials and 20 Rest trials per run). The resting cue was a green circle positioned in the middle of the screen to help them relax, allowing hemodynamic responses to return to baseline. Since our paradigm was designed for BCI communication purposes, the resting period was shortened to 10 seconds, similar to the MI period, which was assumed satisfactory for practical BCI communication. No participants had prior BCI experience, but all participants except ALS-7 and ALS-8 had a single familiarization session before the main recording session.

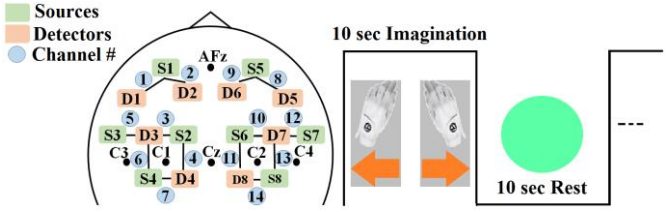

Fig. 1. Left: The fNIRS probe-layout. Right: The motor imagery (MI) task experimental protocol.

C. Data Analysis

1) Signal Preprocessing

The modified Beer-Lambert Law was used to calculate changes in the concentrations of HbO2 and HbR using recorded alterations in the reflected light attenuation [20]. fNIRS data were then band-pass filtered at 0.01-0.09 Hz to eliminate physiological noises caused by respiration (~0.3 Hz), cardiac activities (~1 Hz), and Mayer waves (~0.1 Hz). As fNIRS signal quality can be heavily compromised by the poor coupling of optodes to the head, by optical interference from dense and heavily pigmented hair, the quality of the signal was automatically evaluated through the signal-to-noise-ratio (SNR) of each channel using NIRScout. Further, an exclusion criterion was considered based on a correlation threshold between HbO2 and HbR, indicating a high-level physiological motion artifact [21]. The running correlation between HbO2 and HbR was calculated for each channel, and if it exceeded an 0.5 threshold, or was strictly -1, the channel was discarded. Data was initially segmented into 10-sec trials of LMI, RMI, and Rest, according to the stimulus presentation time. To discriminate MI-HR from Rest-HR, trials were combined to form two sets, with 60 trials for each condition of MI-HR and Rest-HR, representing the two classes. Individual MI tasks that contained artifacts were automatically rejected based on subject-specific thresholds. To analyze the spatio-temporal characteristics of the complete hemodynamic response pattern, MI trials were concatenated to the following Rest trials in a single MI-Rest trial (10 sec LMI/RMI, followed by 10 sec Rest) to form a total of 60 MI-Rest trials. Due to fNIRS oscillatory nature, MI task data was then down-sampled by a factor of 8.6 to account for serial autocorrelations that could impact further hemodynamic response analysis [22].

2) The Generalized Linear Model (GLM) Formulation

An estimation of individualized cortical activation for each MI-Rest trial was performed by fitting the measured hemodynamic response (mHR) corresponding to the MI-Rest trial to a generalized linear model (GLM) using a robust regression algorithm [23]. The GLM was formulated according to [23] using the following equation:

$$mHR_j^i = \beta_j^i . dHR + \psi_j^i . 1 + \varepsilon_j^i \quad (1)$$

where $mHR_j^i \in R^{N\times 1}$ is the measured hemodynamic response, corresponding to the j^{th} MI-Rest trial at each channel i, and N is the size of the fNIRS data (N=36 samples for the down-sampled segments of 10 sec MI and 10 sec Rest). mHR is modeled as a linear combination of the desired (ideal) hemodynamic response (dHR), β is the unknown regression coefficient quantifying the dHR magnitude, ψ is a coefficient to compensate for the baseline drift, $1\epsilon R^{N\times 1}$ is the constant term to model the baseline, and ε is the "error" or "residual" term minimized in fitting the measured mHR to the dHR.

Cortical activation was evaluated based on the statistical comparison of the mHR to the dHR. The dHR is typically modeled as a linear time-invariant system, computed by convolving the stimulus pattern, defined as a boxcar-shaped function, $Box(k)$, where k references time samples (i.e., 10 sec MI task and 10 sec Rest), with the canonical hemodynamic response function (cHR) as follows:

$$dHR(k) = \sum_{n=-\infty}^{\infty} Box(k)\,.\,cHR(\,k-n) \qquad (2)$$
$$Box(k) = 0, if\ k\ \epsilon\ Rest$$
$$1, if\ k\ \epsilon\ MI$$

The cHR is a specific time series shape generated by a statistical parametric mapping (SPM) consisting of a linear combination of two gamma functions (Γ) as shown below [24]:

$$cHR(k) = \left(\frac{k^{\alpha_1-1}\cdot\gamma_1{}^{\alpha_1}\,.\,e^{-\gamma_1 k}}{\Gamma(\alpha_1)} - c\,\frac{k^{\alpha_2-1}\cdot\gamma_2{}^{\alpha_2}\,.\,e^{-\gamma_2 k}}{\Gamma(\alpha_{21})}\right) \qquad (3)$$

where α_1 =6 sec represents the delay of the hemodynamic response relative to the MI onset, $\gamma_1 = \gamma_2 = 1$ sec respectively represent the dispersion of hemodynamic response and the undershoot, $\alpha_2 = 16$ sec represents the delay of the undershoot relative to MI onset, and $c = 1/6$ represents the amplitude ratio of the undershoot to the peak response. The gamma function (Γ) acts as a normalization parameter, and our kernel length is 20 sec. Robust regression estimates of β weights were obtained to indicate dHR activity strength and used in further analysis. Note that the cHR parameters followed previous studies [23].

Based on the main patterns of the fNIRS hemodynamic responses for motor tasks in healthy individuals, two main responses could be identified: a typical response of a delayed increase in HbO2, and a slower, lower amplitude decrease in HbR [25], and/or an inverted response, characterized by a decrease in HbO2 and/or an increase in HbR [26]. As the MI-hemodynamic responses (MI-HR) characteristics of ALS and the respective inter-subject variability are still under evaluation, we performed a temporal-response evaluation prior to the GLM analysis, where each trials' MI-HR pattern was evaluated to determine whether the HbO2 response was typical or inverted. Following this evaluation, the GLM was applied based on the conventional cHR for the typical response, or an inverted cHR for the inverted response. In this way, we ensured that our GLM was built based on subject-specific cortical activations for both response shapes, highlighting individualized differences.

3) Brain Activation Maps

A key factor in designing a robust BCI based on MI responses is to detect a satisfactory level of cortical activation in response to the task and to investigate its consistency across trials. In this study, a statistical *t*-value comparison between the measured data for each MI-Rest trial and the dHR was adopted based on the estimated β weights obtained from our GLM model. The *t*-value was defined as the ratio of the regression coefficient to its standard error [23], as shown follows:

$$t_j^i = \frac{\beta_j^i}{SE(\beta_j^i)} \qquad (4)$$

where SE is the standard error of the estimated coefficient to measure the size of the difference between the mHR_j^i of channel j and the dHR. The *t*-values for HbO2 responses were calculated for individual MI-Rest trials and used to create brain activation maps to illustrate the statistically significant active channels across trials. Significantly active channels were defined through a one-sample *t*-test using a *t*-value based channel selection approach [27]. The selection reliability was assessed using *t*-values above the critical *t*-value (t_{crt}=1.69), computed based on the degrees of freedom for the data (N-1=35) and the statistical significance level (α= 0.05). A significant positive *t*-value ($t>t_{crt}$) indicates that the channel is significantly active, i.e., highly correlated with the dHR, whereas a negative *t*-value indicates an inactive channel. To keep equal standards across trials, the *t*-values were normalized within the range of 0-1 using the following equation:

$$a' = \frac{a-\min(a)}{\max(a)-\min(a)} \qquad (5)$$

where a denotes the actual *t*-value, a' the normalized *t*-value, and $\min(a)$ and $\max(a)$ the minimum and maximum *t*-values across the trials.

4) Classification Procedure

Linear SVM, commonly used to classify hemodynamic responses, were used to evaluate the performance of each subject and the ability to discriminate between their MI-HR and Rest-HR responses using 5-fold cross-validation. For channel selection, the *t*-value-based channel selection approach explained in section II.C.3, was adopted, where at most eight significantly active channels ($t>t_{crt}$) out of fourteen were considered for classification [27]. The *t*-value-based channel optimization used only the training set to avoid biased estimation. For each training set, the *t*-values obtained from the GLM analysis were averaged across the training trials to determine the overall significantly active channels. Incremental sets of significantly active channels starting from a single channel (the most significantly active) up to a maximum of eight significant channels were then selected and considered for further analysis.

In order to distinguish MI-HR from the Rest-HR condition, eight discriminative features commonly used in fNIRS-BCI studies were extracted from each HbO2 and HbR response, corresponding to MI and Rest trials. The features included signal mean ($Mean_{HbO2}$, $Mean_{HbR}$), signal maximum (Max_{HbO2}, Max_{HbR}), signal slope ($Slope_{HbO2}$, $Slope_{HbR}$), signal variance (Var_{HbO2}, Var_{HbR}), signal skewness ($Skew_{HbO2}$, $Skew_{HbR}$), signal kurtosis ($Kurt_{HbR}$, $Kurt_{HbR}$), and the difference between the mean and the minimum (DMM_{HbO2}, DMM_{HbR}). In addition, as the MI-hemodynamic response (MI-HMR) for ALS is still under evaluation, and considering individual MI-HR differences [28], an additional feature was proposed to account for subject-specific hemodynamic characteristics instead of typical cHR. This was inspired by promising prior results in which the β coefficients were adaptively estimated for real-time fNIRS imaging and used as features for classification [29]. For the estimated data-driven β coefficient ($dd\beta$) feature, the GLM model formulation was built based on subject-specific, data-driven hemodynamic responses ($ddHR$) within a 10 sec period (i.e., only the MI period), instead of the typical 20-sec period used in the dHR. The subject-specific $ddHR$ was defined as the overall average MI-HR activation across all the MI trials in the training set to specifically capture individual hemodynamic patterns. Estimated $dd\beta$ regression coefficients for each trial were then used as additional features representing the cortical activation strength for each channel.

Features were optimized for each subject through the 5-fold cross-validation iterative procedure to ensure that the subject-specific combination of features that contains the most discriminative information was properly identified. To do so, all possible combinations of two to eight of the eight features

(246 possible combinations, i.e., $\binom{8}{2}+\binom{8}{3}+\ldots+\binom{8}{8}$, possible one- to eight- channels selected based on the previously explained *t*-value brain activation procedure, and time-windows ([0-10] sec, and [2-7] sec), were considered for each subject's HbO2, HbR, and combined HbO2 and HbR fNIRS responses. If both HbO2 and HbR data were used, the feature combinations were created and concatenated from both signals. The choice of time windows was guided by promising results from previous studies, reporting that confining the time window to [2-7] sec post-stimulus within the overall 10 sec MI task period improves classification performance, as typical hemodynamic responses lag the neuronal event by ~2 sec and take ~5 sec to reach peak value [14]. Notably, the subject-specific $ddHR$ necessary to estimate the $dd\beta$regression coefficients was calculated by averaging the MI trials for each training set over the selected significantly active channels. Results are reported for optimal subject-specific classification outcomes out of all possible classification problems for each subject (3 fNIRS response combinations, 246 feature combinations, 2 time-windows, and up to 8 possible sets of selected channels). The performance was evaluated using 2 metrics: accuracy (Acc) and the F-score. An experimental analysis to investigate the effect of the number of selected channels and the length of time window on optimal classification performance was implemented and reported in the supplementary material (see Fig. S1). As this study primarily focused on the classification of MI vs. Rest to verify hemodynamic-based MI activation for ALS, the proposed methods focused on characterizing the spatio-temporal characteristics of MI-Rest trials (combining LMI and RMI) for optimal classification. However, considering the practical importance of discriminating LMI vs. RMI, preliminary results were also reported in the supplementary material to avoid distracting from the main focus of this work (see Table S1).

5) Correlation Analysis

Correlation between classification accuracies corresponding to each ALS patient and their clinical scores (ALSFRS-R) was performed using the Spearman correlation coefficient (rho) with a significance level of α= 0.05. This analysis assessed the effect of patients' disability levels on BCI performance.

III. Results

In order to show the consistency of MI-HR cortical activation across trials, GLM analysis results are displayed in Fig. 2, which shows brain activation maps for ten representative MI-Rest trials, and the averaged map showing overall activation across the ten trials, for each participant. The brain activation maps show the normalized *t*-values within the range of 0-1, for illustration only. The normalized *t*-values represent the level of activation of each channel, encoded by color intensity. The numbers in the maps refer to channel numbers. We observed consistent significant ($t>t_{crt}$) cortical activation for all subjects across most trials, which indicates the reliability of MI-HR as a control signal for a single trial BCI for ALS patients. However, cortical activation topographies were not consistent between subjects, except for primary motor cortex activation. This indicates variable spatial characteristics of MI-HR across ALS subjects, and highlights the importance of determining subject-specific active channels for an improved BCI performance.

Fig. 3 illustrates the averaged brain activation maps (actual *t*-values) across all MI-Rest trials. Subject-specific significant activation patterns were observed for all subjects, with different cortical activation patterns for each individual. ALS-1 showed significant bilaterally diffused activation over the pre/frontal and motor cortex, with significant *t*-values occurring at CH8 (*t*-value=2.43), CH6 (*t*-value=2.36), CH1 (*t*-value=2.37), CH2 (*t*-value=2.13), CH12 (*t*-value=2.05), CH7 (*t*-value= 2.00), and CH9 (*t*-value= 1.95). For ALS-2, the most significant activation was localized in the dominant (left) hemisphere in the motor cortex CH3 (*t*-value=4.80), CH5 (*t*-value=3.91), particularly the area for right-hand movement (C1 and C3) and the pre/frontal cortex CH1 (*t*-value=4.82), and CH2 (*t*-value=4.39). Slightly lower levels of activation were centered in the motor cortex (surrounding Cz) in CH4 (*t*-value=3.45) and CH11 (*t*-value=3.91). ALS-3's activity was bilaterally localized in both the pre/frontal and primary motor areas, where CH12 (*t*-value=3.24), CH5 (*t*-value=3.10), and CH3 (*t*-value=2.44) surrounding the cortical hand-areas in both hemispheres (C4 and C3, respectively) were the most activated areas. ALS-3 also had the highest pre/frontal activation at CH1 (*t*-value=2.68) and CH8 (*t*-value=1.93). For ALS-4, the most significant activation was observed in CH11 (*t*-value=3.57), covering the central-right primary motor cortex (C2 and Cz) along with CH9 (*t*-value=2.70), and CH2 (*t*-value=2.59) in the pre/frontal cortex. For ALS-5, activation was highly localized in the primary motor cortex, CH3 (*t*-value=5.84), and CH5 (*t*-value=4.93) surrounding the right-hand area (C1 and C3), in the dominant (left) hemisphere, while in the pre/frontal cortex, CH8 (*t*-value=5.31), and CH9 (*t*-value=5.28), covering the pre/frontal cortex in the opposite (right) hemisphere, were the most activated locations in the right hemisphere. For ALS-6, the activity was more localized in the left-hand area in the dominant (right) hemisphere, and more diffused in the left hemisphere. Specifically, CH12 (*t*-value=5.02) was the most significantly activated, along with CH4 (*t*-value=4.57), CH5 (*t*-value=4.21), and CH1 (*t*-value=4.05), in both the primary motor and pre/frontal cortex, respectively. For ALS-7, activity was more diffused bilaterally in both the pre/frontal and the primary motor cortex, with CH12 (*t*-value=3.88), CH10 (*t*-value=3.42), CH1 (*t*-value=3.46), CH5 (*t*-value=3.40), CH2 (*t*-value=3.34), CH6 (*t*-value=3.21), and CH3 (*t*-value=3.00) showing the highest activation levels. For ALS-8, the activity was mainly localized on the right primary motor cortex in CH13 (*t*-value=4.55) and CH12 (*t*-value=3.75) surrounding the left-hand area (C2 and C4). The right pre/frontal cortex also had a high activation level, primarily located around CH8 (*t*-value=3.69).

Fig. 4 illustrates the overall normalized grand-average of HbO2 and HbR responses for each subject over all of the MI-Rest trials for representative significantly active channels. The figure illustrates the responses starting 5 sec prior to the MI stimulus, followed by the 20-sec MI-Rest trial. In general, we observed a variability in the temporal characteristics of hemodynamic responses both at the subject level (i.e., across subjects) and at the channel level (i.e., within each subject). Comparing subject-specific representative significantly active channels, individual variations in the temporal characteristics of the hemodynamic responses were observed in the onset of the rise and the peak time. For ALS-2, ALS-4, and ALS-6, the HbO2 rise started ~2 sec after MI stimulus onset.

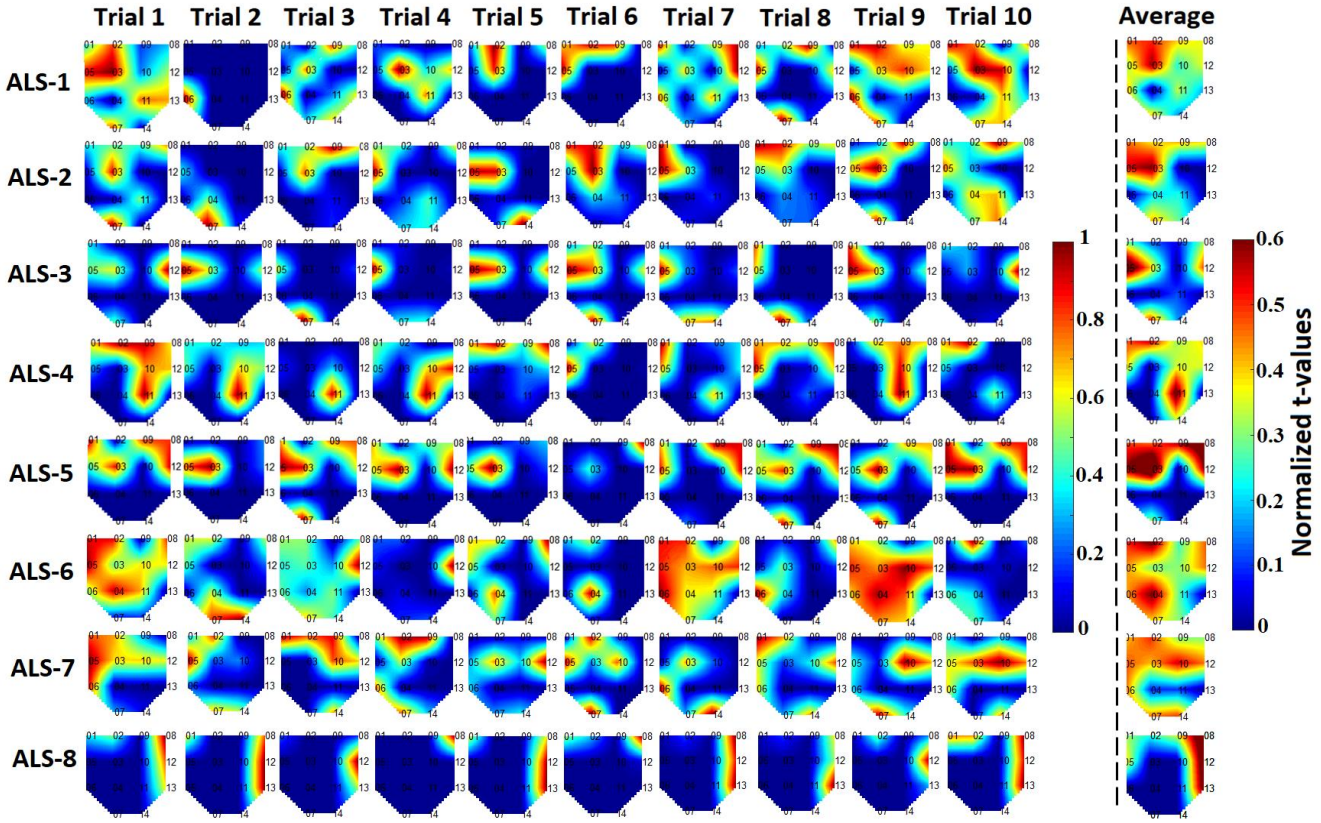

Fig. 2 Brain activation maps for ten representative MI-Rest trials (including both LMI and RMI) for all subjects to show the consistency of MI activation for ALS patients across trials. The channel locations are displayed as numbers on the plots. The maps showed the normalized *t*-values based on the GLM analysis, and the color bar shows the level of brain activation. The last column on the right represents the averaged brain activation map across the ten selected trials.

For ALS-3 and ALS-5, the HbO2 response had a relatively early rise, starting almost 0.5 sec after MI stimulus onset. However, for ALS-1 and ALS-7, the HbO2 rise was delayed, starting ~3 sec and ~4 sec, respectively. These subjects' fNIRS response, illustrated in Fig. 4, was a typical pattern in which the HbO2 response was coupled with a decrease in HbR response at approximately the same time of the HbO2 rise. We further observed individual variations in a few individuals' HbO2 response peak times, starting ~5 sec (for ALS-4), ~6 sec (for ALS-3, ALS-5, and ALS-6), ~8 sec (for ALS-1, and ALS-7), and ~9 sec (for ALS-2). For almost all subjects, the HbR response reached its lowest level later than its peak HbO2 response. The lowest HbR responses were ~8 sec (for ALS-5), ~11 sec (for ALS-1), ~14 sec (for ALS-6), and ~15-sec (for ALS-2 and ALS-4), relative to MI stimulus onset. For ALS-3 and ALS-7, the HbR response reached the lowest level ~ 7 and ~8 sec, respectively; however, their responses were extended along the Rest period (i.e., there was less difference between the response in the MI period and the Rest period). For ALS-3, the HbR response maintained a slightly flat decrease, before both HbO2 and HbR responses slowly returned to baseline at the end of the Rest period. For ALS-7, the HbO2 response had a second peak ~14 sec, while the HbR response reached another low level ~15 sec after the MI stimulus onset. Finally, the observed hemodynamic response pattern for ALS-8 was inverted. His HbO2 response started decreasing ~2 sec prior to stimulus onset, reaching its lowest level ~1.5 sec, while the HbR started increasing around the stimulus onset, peaking ~5 sec, as illustrated in Fig. 4.

Notably, we observed variability in response patterns (i.e., typical versus inverted) at the channel level for several subjects (ALS-1, ALS-2, ALS-3, and ALS-7), while one subject (ALS-8) showed inverted responses in all channels, and three (ALS-4, ALS-5, and ALS-6) had typical patterns in all channels. Fig. 5 illustrates the overall normalized grand-average of HbO2 and HbR inverted responses, observed for some subjects, averaged across MI-Rest trials for representative significantly active channels. For ALS-1, and ALS-2, the HbR response started increasing ~1.5 sec and ~2 sec after the MI stimulus onset, while their HbO2 response had a relatively early decrease, starting almost 2 sec before stimulus onset. For ALS-3, HbR started increasing ~3 sec, while the HbO2 response of the Rest

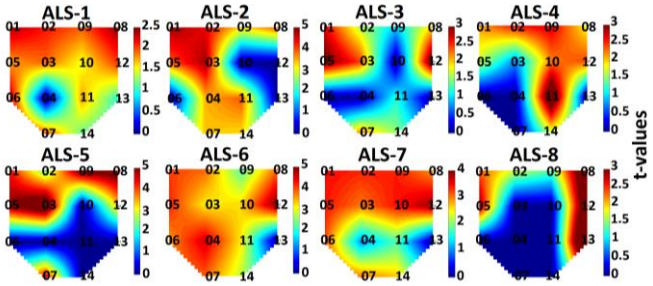

Fig.3 Brain activation maps for each subject averaged over all of the MI-Rest trials to show the overall subject-specific activation levels. The channel locations are displayed as numbers on the plots. The maps show the actual *t*-values (averaged over all the MI-Rest trials) based on the GLM analysis, and the individual color bars show the averaged level of brain activation for each subject (significant activation: *t*-value>t_{crt}=1.69).

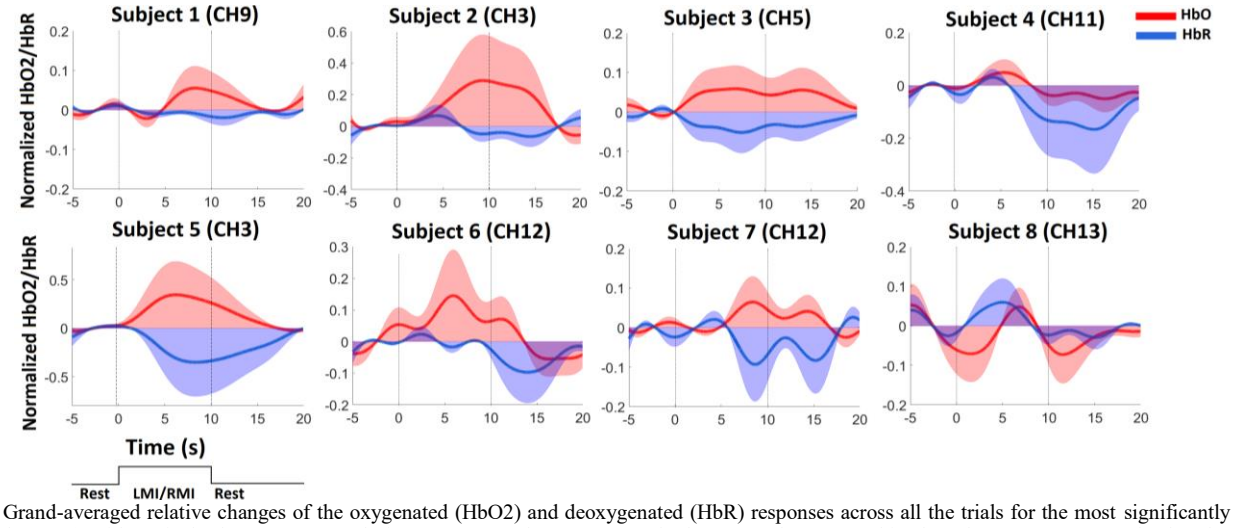

Fig. 4 Grand-averaged relative changes of the oxygenated (HbO2) and deoxygenated (HbR) responses across all the trials for the most significantly active channels ($t>t_{crt}$) with typical HbO2 responses during MI-Rest task (10 sec MI, both LMI and RMI combined, and 10 sec Rest). Each plot shows the hemodynamic response from 5 sec prior to the MI stimulus onset to 20 sec post-stimulus.

period. For ALS-7, the HbR response started increasing around 5 sec, coupled with an HbO2 decrease around 7 sec relative to MI onset. Individual variations were also observed in response peak and trough times. For ALS-1, the HbR response peaked around 6.5 sec, and the HbO2 response reached its lowest level about 2.5 sec after the stimulus onset. Similarly, for ALS-2, the HbR response peaked around 6.5 sec, while the HbO2 reached its lowest level around 1.5 sec post-stimulus.

For ALS-3 and ALS-7, a relatively late peak of HbR response appeared around 11 sec and 17 sec, respectively. ALS-7's HbO2 response reached its lowest level around 16 sec. For both ALS-3 and ALS-7, the observed inverted response was extended along the Rest period, similar to their typical response, and differences between responses during MI and Rest conditions are minimal for these two subjects maintained a slightly flat pattern, below HbR, before both HbO2 and HbR responses slowly returned to baseline at the end

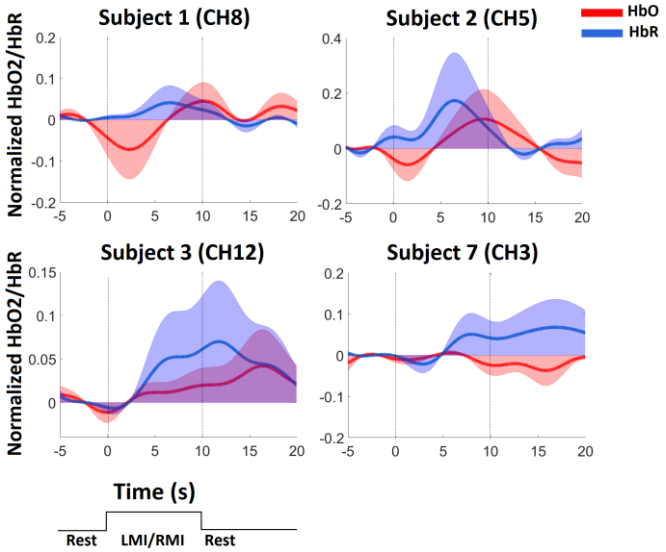

Fig. 5 Grand-averaged relative changes of the oxygenated (HbO2) and deoxygenated (HbR) responses across all the trials to illustrate the observed inverted responses for the most significantly active channels ($t>t_{crt}$) for four ALS subjects performing a MI-Rest task (10 sec MI, both LMI and RMI combined, and 10 sec Rest). Each plot shows the hemodynamic response from 5 sec prior to the MI stimulus onset to 20 sec post-stimulus.

Table II shows subject-specific optimized classification features, parameters, and performance. For each subject, the optimal number of active channels (up to 8), the optimal time window relative to the stimulus-onset ([0-10] sec, or [2-7] sec), the most discriminative fNIRS responses (HbO2, HbR, or both), and the optimal feature combination (of 2 to 8 features) used to obtain the maximum classification performance are displayed. The performance metrics used averaged 5-fold cross-validation classification accuracy and F-score.

The classification outcomes show that all participants in this study were able to use their MI-HR to successfully reach an acceptable BCI performance. The performance metrics reported in Table II utilized subject-specific features, channels, and parameters related to each ALS patient's individual hemodynamic responses. Overall, ALS subjects achieved an average classification accuracy of 85.4%±9.8% and an average F-score of 0.87±0.09, reaching a maximum accuracy of 98.6% and an F-score of 0.99 (for ALS-4) using a [2-7] sec response window relative to imagination onset, and only two features (Max and Slope). The minimum accuracy reached was 73.8%, with an F-score of 0.83 for ALS-1, who was in late-stage LIS. It is worth noting that using data from both HbO2 and HbR optimized the performance for almost all subjects (except ALS-1 and ALS-2). Similarly, confining the time window to [2-7] sec post-stimulus within the 10 sec MI task period improved the classification performance for three subjects (ALS-4, ALS-6, and ALS-7). In addition, a combination of two features was sufficient to obtain a satisfactory performance for most subjects, while the maximum number of features used was four (for ALS-2) out of all of the possible combinations (i.e., sets of 2 to 8 features) investigated in this study. As for the number of channels, the optimal subject-specific number of channels varied across subjects from a single channel to 8 channels.

Fig. 6 illustrates the discriminative ability of the features by comparing their frequencies in the optimized subject-specific features across all subjects. Signal Max was selected as an optimum feature for half of the subjects, and Mean, Slope, Kurt, and $dd\beta$ were included in the combination for three subjects, as shown in Table II and Figure 6. Signal Skew and DMM were included in optimizing the performance for two subjects (ALS-

Table II
OPTIMIZED SUBJECT-SPECIFIC CLASSIFICATION PARAMETERS, FEATURES, AND PERFORMANCE.

Subject Number	*Number of Channels*	*Time Window (sec)*	*fNIRS Signal*	*Optimal Feature Combination*	*Acc (%)*	*F-Score*
1	5	0-10	HbO2	Kurt, DMM	73.8	0.83
2	8	0-10	HbO2	Slope, Mean, Max, Kurt	88.6	0.89
3	5	0-10	HbO2, HbR	Skew, ddβ	74.4	0.74
4	8	2-7	HbO2, HbR	Slope, Max	98.6	0.99
5	3	0-10	HbO2, HbR	Mean, Kurt	95.0	0.95
6	6	2-7	HbO2, HbR	Slope, Max, Skew	92.9	0.93
7	6	2-7	HbO2, HbR	Max, ddβ	76.4	0.74
8	1	2-7	HbO2, HbR	Mean, ddβ	83.3	0.88
Average	~5	-	-	-	**85.4±9.8**	**0.87±0.09**

3 and ALS-6) and a single subject (ALS-1), respectively.

Our Results did not identify any statistical correlation between the ALS patients' classification accuracy and their ALSFRS-R score (rho=0.12, p=0.79). This is consistent with previous studies related to BCI performance evaluation for ALS patients [30]. While the minimum classification accuracy in this study (73.8%) corresponded to the subject with the lowest ALSFRS-R score (ALS-1), i.e., the highest level of disability, this did not hold for other subjects, such as ALS-4, who had a relatively high degree of disability (ALSFRS-R=7), but achieved the highest accuracy in this study (98.6%).

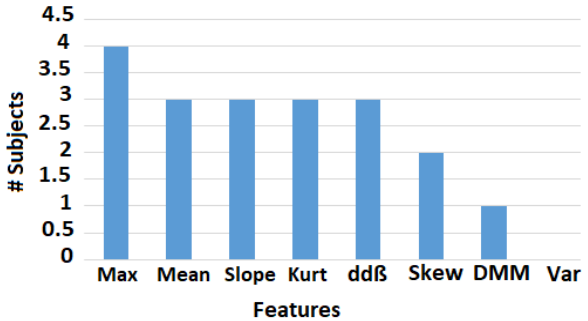

Fig. 6 Histogram showing the selection frequencies of the features in the optimized subject-specific feature sets.

IV. Discussion

The complex neurobiological substrates underlying ALS, along with the variabilities commonly identified in human fNIRS hemodynamic responses [26], can result in potential subject-specific hemodynamic response changes, adding further challenges to the practical design of fNIRS-based BCI systems for these patient. In the present work, we proposed a subject-specific data-driven approach to optimize fNIRS-based BCI performance for ALS patients. Our findings demonstrated that regardless of their disability level, ALS patients can reach a satisfactory level of performance (>85%), indicating an acceptable level of separability in a binary BCI.

Despite inter-individual variations, our findings showed overall consistent intra-individual cortical activation across trials. Relatively limited inconsistency in the intra-individual cortical topographies can be attributed to general hemodynamic variations commonly reported for fNIRS signals [31]. The observed consistency across trials demonstrated that MI-HR can be utilized as a potential input for a practical MI-BCI. Furthermore, an overall significant level of cortical activation was observed for all subjects, indicating that MI-HR can be identified in ALS patients using fNIRS signals. As expected, the overall activation across all trials for each subject revealed individual cortical spatial distribution, with both the pre/frontal and primary motor cortices having significant bilaterally-localized activation in almost all subjects. This is consistent with the previous findings indicating pre-frontal [32] and primary motor activation [11], [33] during MI tasks that follow the same organization as ME, and is not due to muscle activity. Moreover, as previously reported [34], the spatial distribution of MI-HR are more bilateral rather than contralateral when compared to ME, consistent with our results, showing bilateral spatial distribution of activation for most subjects.

Evaluating the individualized temporal characteristics of the MI-HR, our results showed that the main pattern identified for most subjects was a typical MI-HR (i.e., increase in HbO2 and decrease in HbR) associated with the MI stimulus onset. However, the observed temporal characteristics of the typical MI-HR varied across subjects. It is worth noting that only one subject (ALS-8) had an inverted MI-HR in all channels. This is consistent with previous fNIRS-based MI studies, observing inverse oxygenation responses during ME and MI tasks [26], [35], [36], more likely associated with the MI rather than ME, as indicated in [26]. Interestingly, in our study, both typical and inverted patterns were observed in different channels for half of the subjects. This suggests fNIRS response variability on the channel level, within the same subject, and emphasizes the need for personalized feature sets, capturing subject-specific spatial hemodynamic variations. Moreover, the inconsistency of hemodynamic patterns (i.e, typical or inverted) across channels might explain why some subjects who had more consistent patterns across channels (e.g., ALS-5 and ALS-8) needed fewer channels for optimized BCI performance than other subjects (see Table II). However, this was not the case for some subjects (ALS-4 and ALS-6), whose typical patterns were also consistent across channels, but more channels were required to reach their optimal outcomes. Whether this could be explained by variability in the temporal responses across channels, or distinct spatial activations, requires further investigation.

Generally, fNIRS measures brain activity indirectly based on the cortical neurovascular coupling. In typical responses, the rise of HbO2 levels has been interpreted as the result of the increase in cerebral blood flow (CBF) to active regions stimulated by the increase in neural activity. Typically, this physiological response remains as long as the CBF overcompensates for tissues' energy demand in the active areas. Hence the typical response observed in several subjects in this study is explained by localized changes in their cortical

activities through blood oxygenation levels, before slowly returning to baseline upon the task ends [25]. The physiological mechanisms underlying inverted hemodynamic responses have not yet been clearly explained. Holper et al. [26] reported that the inverted response observed in some healthy subjects, during simple and/or complex MI tasks, is likely due to individual variations in the cognitive mechanisms underlying simple vs. complex tasks. A behavioral interpretation was suggested in the context of the empirical relation [37] (i.e., the Yerkes-Dodson law) between attention and performance, speculating that the inverse response might be related to the increased mental load of MI, to the point where the engaged cortical area starts deactivating. The inverted hemodynamic patterns observed in five subjects throughout this study support these findings, and suggest a different spatial mechanism underlying their MI experiences. However, individual variations in fNIRS responses and their relationship with underlying cognitive mechanisms in fNIRS-based BCI studies requires further investigation. Another plausible interpretation is based on similar fMRI findings describing negative BOLD responses [38], suggesting that the inverted response can also reflect local neural deactivation due to a decrease in CBF as a result of a decrease in neural activation. Considering the comparison between fMRI and fNIRS, the increase of HbO2 and/or decrease of HbR are commonly suggested to reflect hyper-oxygenation that explains a localized increased cortical activity and, similarly, the decrease of HbO2 and/or increase of HbR reflects hypo-oxygenation during decreased activation [26]. Although the deactivation process during ME and MI has been recently reported in fMRI studies [39], [40], the underlying mechanisms of the negative BOLD remains a matter of debate. Whether the negative responses are of neural origins, or non-neural origins such as "blood steal" phenomena [38], which occurs due to a decrease in CBF adjacent to active regions with increased CBF, requires further investigation.

Our results showed that MI-HR-based BCI performance could be optimized using subject-specific feature sets and classification parameters. The optimal features fundamentally captured discriminative characteristics of morphological variations between MI and Rest conditions from significantly active channels. Notably, the proposed data-driven approach for estimating the $dd\beta$ coefficient was comparable to the Mean and the Slope features, and had a relatively high discrimination ability for a few of subjects. Exploring temporal MI-HR characteristics for these subjects, the difference between their hemodynamic response during MI and Rest period was less prominent in comparison to other subjects. This might explain the reason why conventionally used features, such as maximum, slope, and mean, could not discriminate between MI and Rest. However, modeling a subject-specific $ddHR$ for these subjects and using the $dd\beta$ to estimate the strength of the observed activity could achieve a satisfactory performance for these subjects. This highlights the importance of a subject-specific data-driven approach in fNIRS-based BCI design to achieve acceptable performance, especially for atypical responses, potentially altered by neurological diseases, including ALS. Considering the fact that the fNIRS signal provides information about underlying hemodynamic activities which might be affected by neurological conditions, and the fact that the characteristics of MI-based hemodynamic responses in ALS patients have not been yet thoroughly identified, it is plausible that the hemodynamic response characteristics might not maintain a consistent pattern across ALS patients and/or overtime, within the same subject as their disease progress. The empirical subject-specific data-driven approach proposed in this study minimizes general assumptions about the expected hemodynamic responses, and might represent a solution to this problem, specifically when observed hemodynamic responses do not follow typically expected patterns.

V. LIMITATIONS AND FUTURE DIRECTIONS

The main focus of the present work is limited to spatio-temporal investigations of hemodynamic responses to guide an optimal subject-specific BCI for ALS patients. Our protocol operated primarily as a switch function by offering a binary fNIRS-based BCI control that relies solely on motor imagery (MI vs. Rest) for ALS patients. Preliminary results were further provided for discrimination between LMI vs. RMI in the supplementary part. However, further analysis characterizing spatio-temporal differences in cortical activation between LMI and RMI, as well as optimizing the corresponding parameters for an enhanced classification task are required, to efficiently distinguish between the two MI tasks. Adopting powerful spatial filters, including common spatial patterns (CSP) may also advance the separability of the two classes. Increasing the degrees of freedom (DOF) by investigating MI for other limbs and adding different levels of complexity to the MI task can also improve the efficacy of the proposed BCI for more practical applications. Future analysis will involve testing the feasibility of the proposed methods for a real-time MI BCI scenarios that involve investigating sliding short time windows for an enhanced information transfer rate (ITR), which takes both time and accuracy into account. Future work might also involve characterizing the neuropathological effects of ALS on MI-HR by involving healthy controls. In addition, the statistical power of this study was limited, due to the relative difficulty of recruiting and recording from ALS patients. However, our primary goal was characterization for an optimal BCI use, not the neurophysiological quantification of ALS.

VI. CONCLUSION

This study focused on characterizing and evaluating the spatio-temporal dynamics of hemodynamic responses evoked by MI tasks in order to investigate the feasibility of fNIRS-based hemodynamic responses evoked by MI tasks as a means of BCI control for people with ALS. The proposed methods evaluated the hemodynamic responses and statistically verified MI activation, taking into account both typical and inverted responses. A subject-specific data-driven approach was proposed to accommodate for the individual spatio-temporal characteristics of hemodynamic responses. The proposed data-driven coefficient ($dd\beta$) feature improved the classification performance of subjects with less prominent temporal differences between MI and Rest tasks, suggesting its potential to enhance classification performance for atypical response patterns that might be observed for ALS patients in comparison with conventionally used features (e.g., Max, Mean, and Slope). Despite the observed inter-individual variations in the ALS hemodynamic responses, an optimized performance was

achieved for each subject regardless of their disability level. Our results revealed an average accuracy of 85.4%±9.8%, while no significant correlation was observed between classification accuracies and patients' ALSFRS-R scores. These results highlight the importance of adopting an individualized design that takes into account subject-specific variations, both spatially and temporally, to improve BCI performance for ALS patients.

ACKNOWLEDGMENT

This study was supported by the National Science Foundation (NSF-1913492) and the Institutional Development Award (IDeA) Network for Biomedical Research Excellence (P20GM103430). The authors would like to thank the participants who took part in this study, without whom this study would not have been possible. We would also like to thank the ALS Association, Rhode Island Chapter, for their continuous support, and Alyssa Zisk for proofreading this manuscript.

REFERENCES

[1] G. Pfurtscheller and C. Neuper, "Motor imagery activates primary sensorimotor area in humans," Neurosci. Lett., 1997.

[2] S. Coyle, T. Ward, and C. Markham, "Cerebral blood flow changes related to motor imagery, using near infrared spectroscopy (NIRS)," in World Congress on Medical Physics and Biomedical Engineering, Sydney, Australia, 2003.

[3] A. Vourvopoulos, C. Jorge, R. Abreu, P. Figueiredo, J. C. Fernandes, and S. Bermúdez i Badia, "Efficacy and brain imaging correlates of an immersive motor imagery BCI-driven VR system for upper limb motor rehabilitation: A clinical case report," Front. Hum. Neurosci., 2019.

[4] H. Yuan &B. He, "Brain-computer interfaces using sensorimotor rhythms: Current state and future perspectives," IEEE Trans. Biom Eng, 2014.

[5] A. Kübler, F. Nijboer, J. Mellinger, T. M. Vaughan, H. Pawelzik, G. Schalk, D. J. McFarland, N. Birbaumer, and J. R. Wolpaw, "Patients with ALS can use sensorimotor rhythms to operate a brain-computer interface," Neurology, 2005.

[6] C. Guger, G. Edlinger, W. Harkam, I. Niedermayer, and G. Pfurtscheller, "How many people are able to operate an EEG-based brain-computer interface (BCI)?," IEEE Trans. Neural Syst. Rehabil. Eng., 2003.

[7] S. M. Hosni, R. J. Deligani, A. Zisk, J. McLinden, S. B. Borgheai, and Y. Shahriari, "An exploration of neural dynamics of motor imagery for people with amyotrophic lateral sclerosis," Journal of Neural Eng, 2020.

[8] T. Kasahara *et al.*, "The correlation between motor impairments and event-related desynchronization during motor imagery in ALS patients," BMC Neurosci., 2012.

[9] H. Ayaz *et al.*, "Continuous monitoring of brain dynamics with functional near infrared spectroscopy as a tool for neuroergonomic research: Empirical examples and a technological development," Front. Hum. Neurosci., 2013.

[10] T. J. Huppert, R. D. Hoge, S. G. Diamond, M. A. Franceschini, and D. A. Boas, "A temporal comparison of BOLD, ASL, and NIRS hemodynamic responses to motor stimuli in adult humans," Neuroimage, 2006.

[11] R. Sitaram, H. Zhang, C. Guan, M. Thulasidas, Y. Hoshi, A. Ishikawa, K. Shimizu, and N. Birbaumer, "Temporal classification of multichannel near-infrared spectroscopy signals of motor imagery for developing a brain-computer interface," Neuroimage, 2007.

[12] S. M. Coyle, T. E. Ward, and C. M. Markham, "Brain-computer interface using a simplified functional near-infrared spectroscopy system.," J. Neural Eng., 2007.

[13] L. Holper and M. Wolf, "Single-trial classification of motor imagery differing in task complexity: A functional near-infrared spectroscopy study," J. Neuroeng. Rehabil., 2011.

[14] N. Naseer and K. S. Hong, "Classification of functional near-infrared spectroscopy signals corresponding to the right- and left-wrist motor imagery for development of a brain-computer interface," Neurosci. Lett., 2013.

[15] K. S. Hong, N. Naseer, and Y. H. Kim, "Classification of prefrontal and motor cortex signals for three-class fNIRS-BCI," *Neurosci. Lett.*, 2015.

[16] M. Naito, Y. Michioka, K. Ozawa, Y. I. Ito, M. Kiguchi, and T. Kanazawa, "A communication means for totally locked-in ALS patients based on changes in cerebral blood volume measured with near-infrared light," IEICE Trans. Inf. Syst., 2007.

[17] G. Gallegos-Ayala, A. Furdea, K. Takano, C. A. Ruf, H. Flor, and N. Birbaumer, "Brain communication in a completely locked-in patient using bedside near-infrared spectroscopy," Neurology, 2014.

[18] J. M. Cedarbaum *et al.*, "The ALSFRS-R: A revised ALS functional rating scale that incorporates assessments of respiratory function," J. Neurol. Sci., 1999.

[19] H. Peng, J. Chao, S. Wang, J. Dang, F *et al*., "Single-trial classification of fNIRS signals in four directions motor imagery tasks measured from prefrontal cortex," IEEE Trans. Nanobioscience, 2018.

[20] A. Sassaroli and S. Fantini, "Comment on the modified Beer-Lambert law for scattering media," Physics in Medicine and Biology. 2004.

[21] X. Cui, S. Bray, and A. L. Reiss, "Functional near infrared spectroscopy signal improvement based on negative correlation between oxygenated and deoxygenated hemoglobin dynamics," Neuroimage, 2010.

[22] P. Pinti, F. Scholkmann, A. Hamilton, P. Burgess, and I. Tachtsidis, "Current Status and Issues Regarding Pre-processing of fNIRS Neuroimaging Data: An Investigation of Diverse Signal Filtering Methods Within a General Linear Model Framework," Front. Hum. Neurosci., 2019.

[23] H. Santosa, M. J. Hong, and K. S. Hong, "Lateralization of music processing with noises in the auditory cortex: An fNIRS study," Front. Behav. Neurosci., 2014.

[24] M. A. Lindquist, J. Meng Loh, L. Y. Atlas, and T. D. Wager, "Modeling the hemodynamic response function in fMRI: efficiency, bias and mis-modeling.," Neuroimage, 2009.

[25] D. R. Leff, F. Orihuela-Espina, C. E. Elwell, T. Athanasiou, D. T. Delpy, A. W. Darzi, and G. Z. Yang, "Assessment of the cerebral cortex during motor task behaviours in adults: A systematic review of functional near infrared spectroscopy (fNIRS) studies," NeuroImage. 2011.

[26] L. Holper, D. E. Shalóm, M. Wolf, and M. Sigman, "Understanding inverse oxygenation responses during motor imagery: A functional near-infrared spectroscopy study," Eur. J. Neurosci., 2011.

[27] K. S. Hong, M. J. Khan, and M. J. Hong, "Feature Extraction and Classification Methods for Hybrid fNIRS-EEG Brain-Computer Interfaces," Frontiers in Human Neuroscience. 2018.

[28] G. Jasdzewski, G. Strangman, J. Wagner et al., "Differences in the hemodynamic response to event-related motor and visual paradigms as measured by near-infrared spectroscopy," Neuroimage, 2003.

[29] N. K. Qureshi, N. Naseer, F. M. Noori, H. Nazeer, R. A. Khan, and S. Saleem, "Enhancing classification performance of functional near-infrared spectroscopy-brain-computer interface using adaptive estimation of general linear model coefficients," Front. Neurorobot., 2017.

[30] L. M. McCane, E. W. Sellers, D. J. Mcfarland, J. N. Mak, C. S. Carmack, D. Zeitlin, J. R. Wolpaw, and T. M. Vaughan, "Brain-computer interface (BCI) evaluation in people with amyotrophic lateral sclerosis," Amyotroph. Lateral Scler. Front. Degener., 2014.

[31] K. S. Hong, M. R. Bhutta, X. Liu, and Y. Il Shin, "Classification of somatosensory cortex activities using fNIRS," Behav. Brain Res., 2017.

[32] E. Gerardin, "Partially Overlapping Neural Networks for Real and Imagined Hand Movements," Cereb. Cortex, 2000.

[33] S. C. Wriessnegger et al., "Spatio-temporal differences in brain oxygenation between movement execution and imagery: A multichannel near-infrared spectroscopy study," Int. J. Psychophysiol., 2008.

[34] A. M. Batula, J. A. Mark, Y. E. Kim, and H. Ayaz, "Comparison of Brain Activation during Motor Imagery and Motor Movement Using fNIRS," Comput. Intell. Neurosci., 2017.

[35] L. Holper, N. Kobashi, D. Kiper, F. Scholkmann, M. Wolf, and K. Eng, "Trial-to-trial variability differentiates motor imagery during observation between low versus high responders: A functional near-infrared spectroscopy study," Behav. Brain Res., 2012.

[36] H. Sato, Y. Fuchino, M. Kiguchi, T. Katura, A. Maki, T. Yoro, and H. Koizumi, "Intersubject variability of near-infrared spectroscopy signals during sensorimotor cortex activation," J. Biomed. Opt., 2005.

[37] R. M. Yerkes and J. D. Dodson, "The relation of strength of stimulus to rapidity of habit-formation," J. Comp. Neurol. Psychol., 1908.

[38] A. Shmuel, E. Yacoub, J. Pfeuffer, P. F. Van de Moortele, G. Adriany, X. Hu, and K. Ugurbil, "Sustained negative BOLD, blood flow and oxygen consumption response and its coupling to the positive response in the human brain," Neuron, 2002.

[39] H. Nakata, R. Domoto, N. Mizuguchi, K. Sakamoto, and K. Kanosue, "Negative BOLD responses during hand and foot movements: An fMRI study," *PLoS One*, 2019.

[40] N. Zeharia, U. Hertz, T. Flash, and A. Amedi, "Negative blood oxygenation level dependent homunculus and somatotopic information in primary motor cortex and supplementary motor area," *Proc. Natl. Acad. Sci. U. S. A.*, 2012.